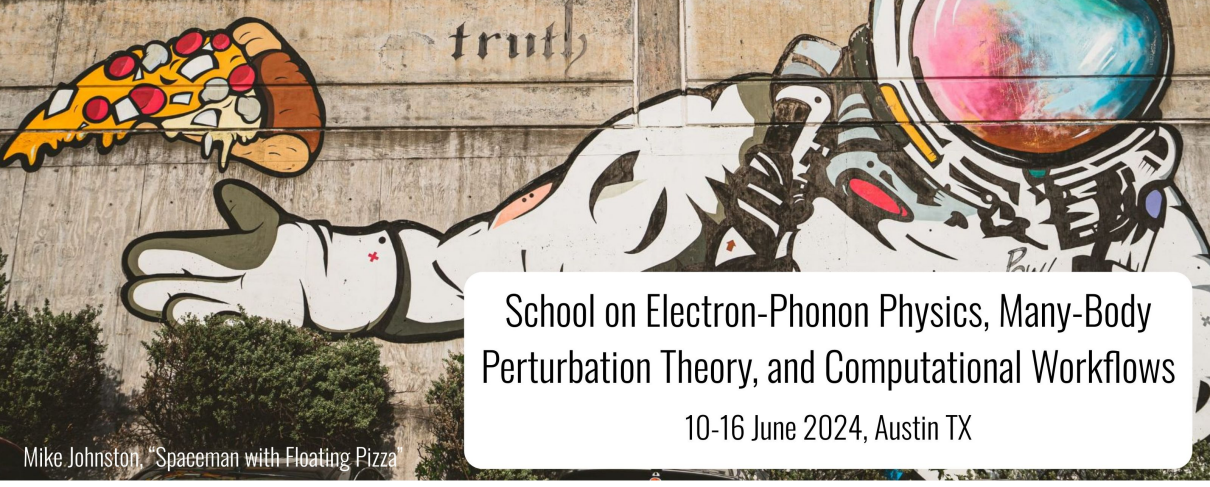

Mike Johnston, "Spaceman with Floating Pizza"

School on Electron-Phonon Physics, Many-Body Perturbation Theory, and Computational Workflows

10-16 June 2024, Austin TX

U.S. DEPARTMENT OF ENERGY

NSF

TACC
TEXAS ADVANCED COMPUTING CENTER

ODEN

Lecture Thu.2

Introduction to polarons

Feliciano Giustino

Oden Institute & Department of Physics

The University of Texas at Austin

Lecture Summary

- Notion of electron self-trapping
- Manifestations of polarons
- DFT calculations of polarons
- Landau-Pekar model
- *Ab initio* polaron equations
- Many-body theory of polarons

Bloch theorem from Lec. Mon.1

Über die Quantenmechanik der Elektronen in Kristallgittern.

Von **Felix Bloch** in Leipzig.

Mit 2 Abbildungen. (Eingegangen am 10. August 1928.)

Die Bewegung eines Elektrons im Gitter wird untersucht, indem wir uns dieses durch ein zunächst streng dreifach periodisches Kraftfeld schematisieren. Unter Hinzunahme der Fermischen Statistik auf die Elektronen gestattet unser Modell Aussagen über den von ihnen herrührenden Anteil der spezifischen Wärme des Kristalls. Ferner wird gezeigt, daß die Berücksichtigung der thermischen Gitterschwingungen Größenordnung und Temperaturabhängigkeit der elektrischen Leitfähigkeit von Metallen in qualitativer Übereinstimmung mit der Erfahrung ergibt.

Einleitung. Die Elektronentheorie der Metalle hat seit einiger Zeit Fortschritte zu verzeichnen, die in der Anwendung quantentheoretischer Prinzipien auf das Elektronengas begründet sind. Zunächst hat Pauli* unter der Annahme, daß die Metallelektronen sich völlig frei im Gitter bewegen können und der Fermischen** Statistik gehorchen, den temperaturunabhängigen Paramagnetismus der Alkalien zu erklären vermocht. Die elektrischen und thermischen Eigenschaften des Elektronengases sind dann von Sommerfeld, Houston und Eckart*** näher untersucht worden. Die Tatsache freier Leitungselektronen wird von ihnen als gegeben betrachtet und ihre Wechselwirkung mit dem Gitter nur durch eine zunächst phänomenologisch eingeführte, dann von Houston**** strenger begründete freie Weglänge mitberücksichtigt. Schließlich hat Heisenberg† gezeigt, daß im anderen Grenzfall, wo zunächst die Elektronen an die Ionen im Gitter gebunden gedacht und erst in nächster Näherung die Austauschvorgänge unter ihnen berücksichtigt werden, das für den Ferromagnetismus entscheidende intermolekulare Feld seine Erklärung findet.

Hier soll ein Zwischenstandpunkt zwischen den beiden oben erwähnten Behandlungsweisen eingenommen werden, insofern, als der Austausch der Elektronen unberücksichtigt bleibt, sie dagegen nicht einfach

* W. Pauli, ZS. f. Phys. **41**, 81, 1927.
** E. Fermi, ebenda **36**, 902, 1926.
*** A. Sommerfeld, W. V. Houston, C. Eckart, ebenda **47**, 1, 1928.
**** W. V. Houston, ebenda **48**, 449, 1928.
† W. Heisenberg, ebenda **49**, 619, 1928.

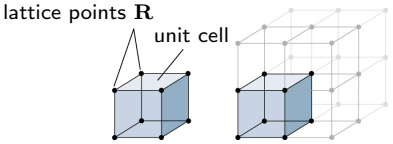

$$\psi(\mathbf{r}) = e^{i\mathbf{k}\cdot\mathbf{r}} u(\mathbf{r}) \text{ with } u(\mathbf{r}+\mathbf{R}) = u(\mathbf{r})$$

Bloch theorem

$$\rho = \frac{c_1}{T}\left(\frac{k_B T}{\hbar C}\right)^6 \int_0^{\hbar C q_D / k_B T} \frac{x^5\,dx}{(e^x-1)(1-e^{-x})}$$

Bloch-Grüneisen formula for electrical resistivity

Landau's question on electron self-trapping

It is well known that in a periodic field an electron can move without resistance. When the lattice is slightly distorted at a point, this only leads to scattering of the electrons at this point. This, however, does not mean the electron is trapped at this point. According to a familiar theorem in wave mechanics this will only be possible if, in addition possible if, in addition to continuous eigenvalues, the distorted lattice would also have discrete eigenvalues. But this is not the case for slight distortions.

Let us consider a free electron, subjected in a certain region to a weak field. we can then demonstrate in accordance with Peierls[1] that the solution of the Schrödinger equation at $E = 0$ has no nodes at weak fields, that is it corresponds to the lowest possible eigenvalue. For, when determining the solution of the Schrödinger equation

$$\nabla^2 \psi = -\frac{2mU}{\hbar^2}\psi \tag{1}$$

for small U in the form

$$\psi = 1 + \chi, \tag{2}$$

where χ is also small, one obtains:

$$\nabla^2 \chi = -\frac{2mU}{\hbar^2}. \tag{3}$$

If U decreases at infinity more rapidly than $1/r^2$, then this equation has a solution finite throughout, and whose values are proportional to those of U. For a sufficiently small U one therefore has $|\chi| < 1$ hence $1 + \chi$ vanishes nowhere. (When denoting the dimension of the region where U is different from zero by a, we find that a discrete eigenvalue can only exist when $mUa^2/\hbar^2$ is of the order of unity.)

An analogous proof is possible for a periodic lattice by taking as starting point the solution corresponding to the lowest eigenvalue which is consequently nodeless for a strictly periodic field, and by writing the "distorted" ψ in the form $\psi = \psi_0 + \chi$.

Hence a small distortion does not yet lead to the possible trapping of the electron. This possibility only exists for large distortions. We can now differentiate between two essentially different cases. For, the energetically most favourable state of the total system may correspond, firstly, to the undistorted lattice and the electron moving about "freely" and, secondly, the electron trapped at a strongly distorted region. In the first case, the electron cannot be trapped at all by the lattice. This situation seems to be realised in the case of diamond. In the second case, the electron can only be trapped when passing over an energy barrier. For, as already stated, in the case of a small distortion, the eigenvalues of the electron are not changed. Hence the energy variation of the total system consists solely in the distortion energy and thus is essentially positive. We must therefore expect that the trapping of the electron is associated with activation effects. This corresponds to the situation in the case of NaCl which cannot be discoloured by X-rays at low temperatures. It would be interesting to verify in this effect the $\exp(-A/kT)$ law and to determine the value of the activation energy A.

REFERENCE

1. R. PEIERLS, *Z. Phys.* 58, 59 (1929).

Electron motion in crystal lattices, Phys. Z. Soviet. 3, 664 (1933)

Landau's reasoning

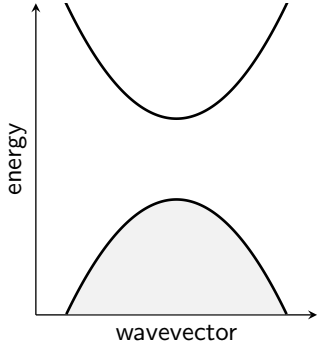

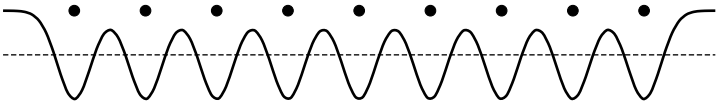

Landau's reasoning

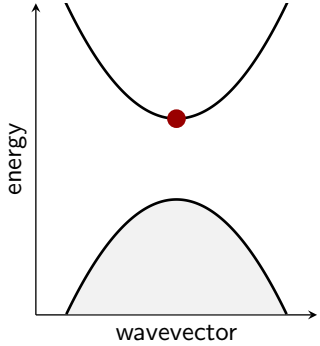

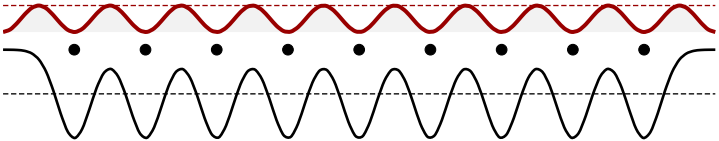

Landau's reasoning

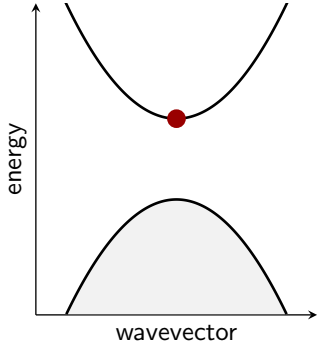

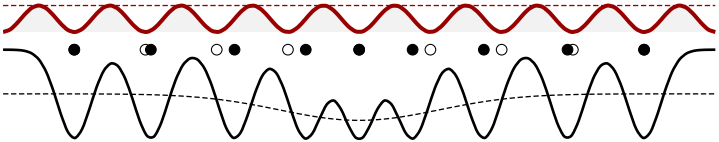

Landau's reasoning

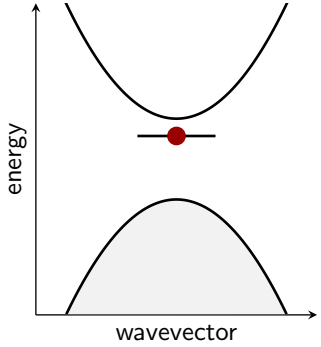

electron **localized** by lattice distortion

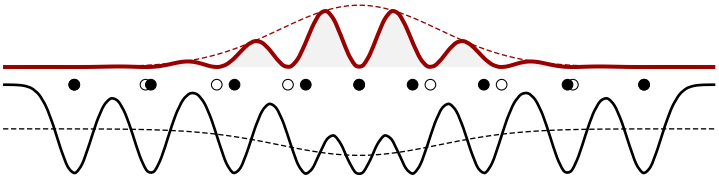

"polaron" © S. Pekar

Transport signatures of polarons

$La_{1-x}Sr_xMnO_3$

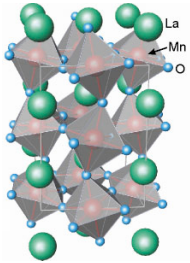

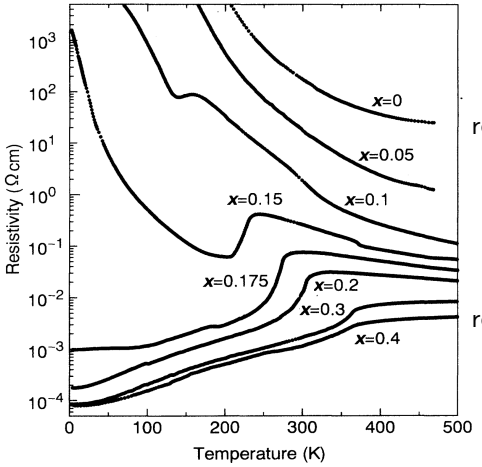

resistivity **decreases** with T

resistivity **increases** with T

→ Lec. Wed.1 Poncé

Right figure from Urushibara, Moritomo, Arima, Asamitsu, Kido, Tokura, Phys. Rev. B 51, 14103 (1995)

Left figure from ESRF Highlights 2001

Transport signatures of polarons

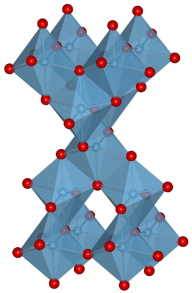

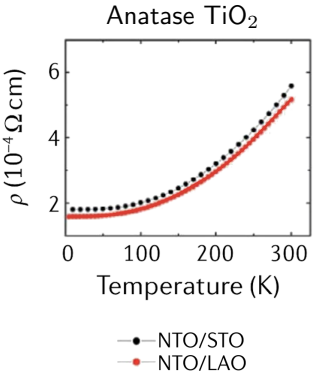

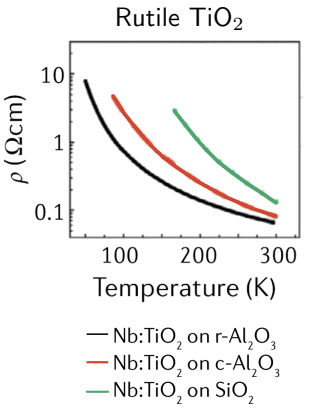

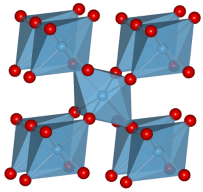

Hall mobility data from Zhang et al, J. Appl. Phys. 102, 013701 (2007)

Scanning tunneling microscopy signatures of polaronss

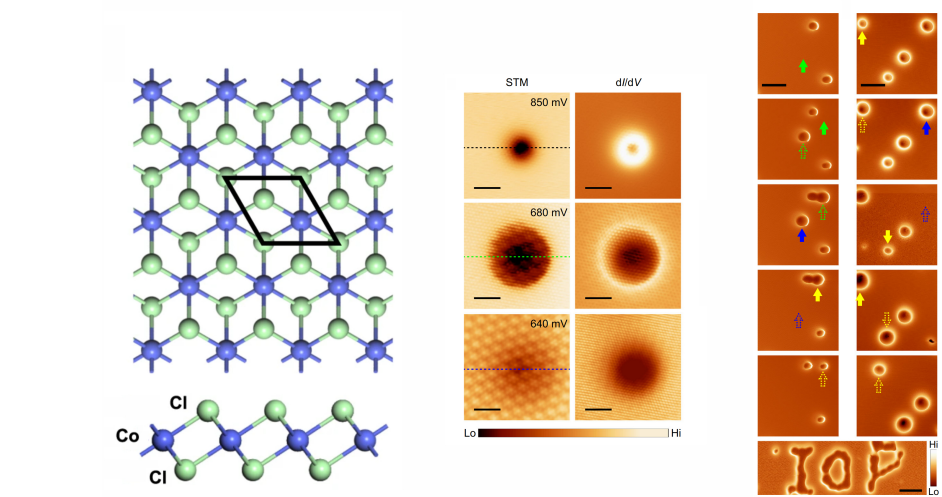

Figures from Liu, Wu, et al, Nat. Commun. 14, 3690 (2023)

The Polaron Zoo

Polaron type	Description	References
Electron or hole polaron	Self-trapped electron or hole coupled with phonons	Reviews[1,137,145,156,318,319]
Large Fröhlich polaron	Long-range electron–phonon interaction, spatially extended	Theory[7,8,85,88], experiments (*n*-doped a-TiO_2)[48]
Small Holstein polaron	Short-range electron–phonon interaction, spatially confined	Theory[9,10,309,310], experiments (UO_{2+x})[15]
Bipolaron	Bound pair of two polarons (Holstein or Fröhlich), similar to a superconducting Cooper pair[169]	Theory[28,320–322] (manganites, cuprates), experiments and DFT ($BaK_xBi_{1-x}O_3$)[313,323,324]
Magnetic (spin) polaron	Small polaron coupled with localized spins	Theory[325,326], experiments and DFT (EuO (REFS[315,327]), Fe_3O4 (REF.[79]), $(La_{1-x}A_x)_{2/3}Ca_{1/3}MnO_3$ (REFS[24,328]))
Jahn–Teller polaron	Polaron stabilized by Jahn–Teller effects	Experiments ($La_{1-x}Sr_xMnO_3$ (REF.[27]), cuprates[28]), experiments and DFT (ABO_3)[329,330], theory[331,332]
Ferroelectric polaron	Polaron stabilized by ferroelectric distortions	Experiments and DFT (halide perovskites)[30,45], DFT ($SrTiO_3$ (REFS[333,334]), strained $BaTiO_3$ (REF.[179]))
Zener polaron	Two spin polarons coupled by double exchange (FM polaron dimer)	Theory (doped manganites)[25], experiments[24,26], HF[335], DFT[177,336]
2D polaron	Polaronic self-trapping confined in 2D	Theory[318,337], experiments (MoS_2)[32], DFT (Hf/ZrO_2)[33]
Polaron exciton (self-trapped exciton)	Bound pair consisting of an electron polaron and a hole polaron	Theory[338–340], experiments (ZnO (REF.[341]), C60 (REF.[54])), review[171] (conjugated polymers)[342]
Dopant/defect polarons	(Small) polarons bound to dopants and defects	Experiments and theory (TiO_2)[46], book[145]
Molecular polaron	Self-trapping caused by short-range chemical bond formation	Theory[343], experiments (DEH molecule)[344], review (conducting polymers)[2]

Table from review article: Franchini et al, Nat. Rev. Mater. 6, 560 (2021)

Polarons in DFT calculations

Electron aded to Li_2O_2 ground state

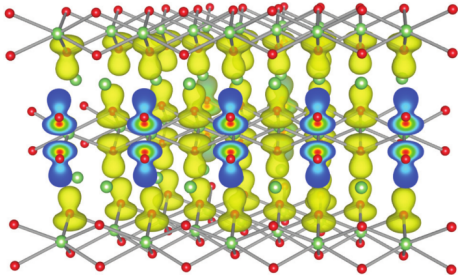

Figure from Feng et al, Phys. Rev. B 88, 184302 (2013)

Polarons in DFT calculations

Electron aded to Li_2O_2 ground state

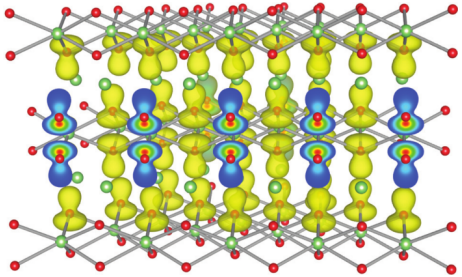

Self-localization after ionic relaxation

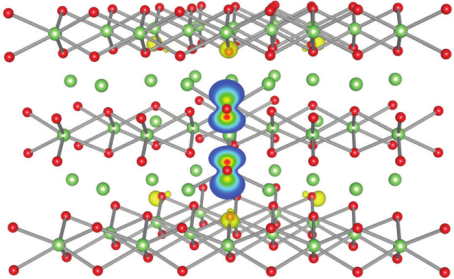

Figure from Feng et al, Phys. Rev. B 88, 184302 (2013)

Polarons in DFT calculations

Electron aded to Li_2O_2 ground state

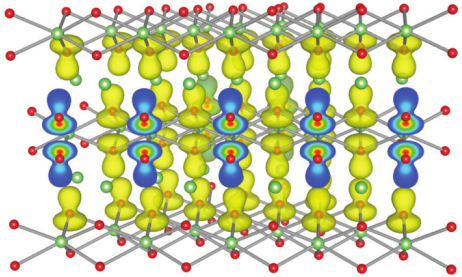

Self-localization after ionic relaxation

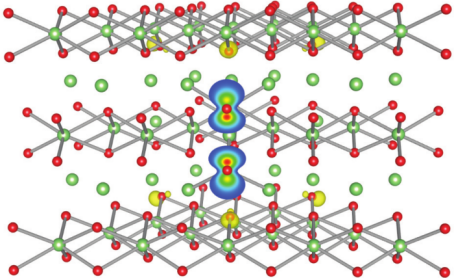

- Formation energy and size sensitive to the XC functional
- Only very small polarons accessible

Figure from Feng et al, Phys. Rev. B 88, 184302 (2013)

Polaron sensitivity to functional in DFT: Hole polaron in MgO

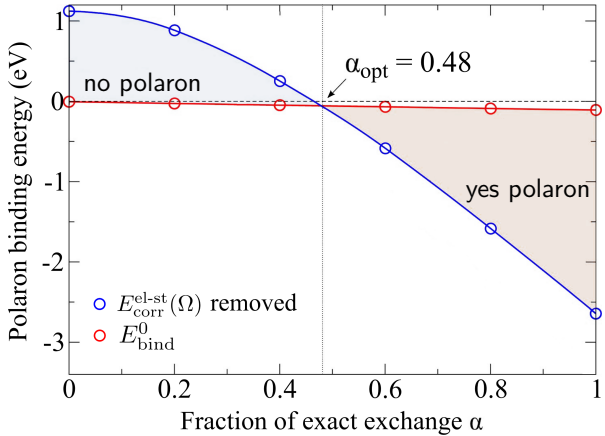

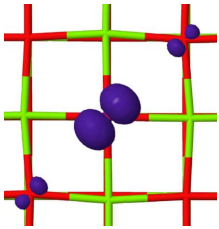

Figures adapted from Kokott, Levchenko, Rinke, Scheffler, New J. Phys. 20 (2018)
See also Falletta, Pasquarello, PRL 129, 126401 (2022) for Koopman's based approaches

Sensitivity to XC functional: Electron polarons in rutile and anatase TiO_2

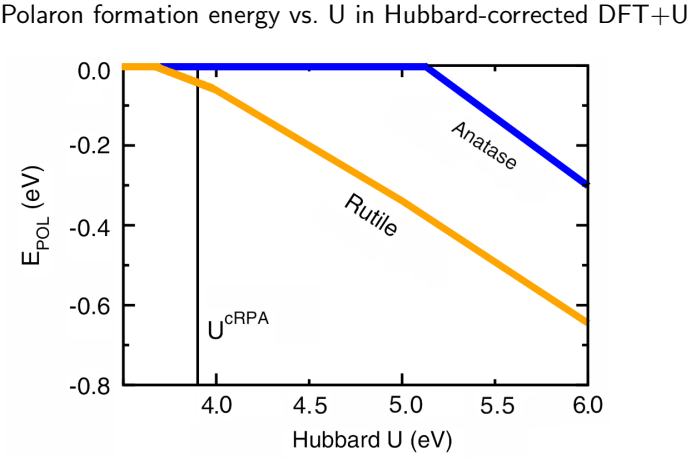

Figures adapted from Setvin, Franchini, Kresse, Diebold, et al, Phys. Rev. Lett. 113, 086402 (2014)

Ground state of the polaron in the Landau-Pekar model

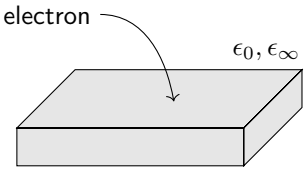

Pekar, Zh. Eksp. Teor. Fiz. 16, 341 (1946); Landau and Pekar, Zh. Eksp. Teor. Fiz. 18, 419 (1948)

Ground state of the polaron in the Landau-Pekar model

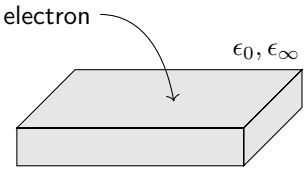

$$E = \frac{\hbar^2}{2m^*}\int d\mathbf{r}\,|\nabla\psi|^2 + \frac{1}{2}\int d\mathbf{r}\;\mathbf{E}\cdot\mathbf{D}$$

Pekar, Zh. Eksp. Teor. Fiz. 16, 341 (1946); Landau and Pekar, Zh. Eksp. Teor. Fiz. 18, 419 (1948)

Ground state of the polaron in the Landau-Pekar model

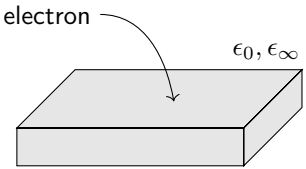

$$E = \frac{\hbar^2}{2m^*}\int d\mathbf{r}\,|\nabla\psi|^2 + \frac{1}{2}\int d\mathbf{r}\;\mathbf{E}\cdot\mathbf{D}$$

$$\nabla\cdot\mathbf{D} = -e|\psi(\mathbf{r})|^2 \qquad \mathbf{D} = \varepsilon_0\epsilon_0\mathbf{E}$$

Pekar, Zh. Eksp. Teor. Fiz. 16, 341 (1946); Landau and Pekar, Zh. Eksp. Teor. Fiz. 18, 419 (1948)

Ground state of the polaron in the Landau-Pekar model

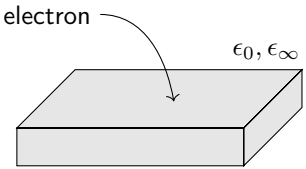

$$E = \frac{\hbar^2}{2m^*}\int d\mathbf{r}\,|\nabla\psi|^2 + \frac{1}{2}\int d\mathbf{r}\;\mathbf{E}\cdot\mathbf{D}$$

$$\nabla\cdot\mathbf{D} = -e|\psi(\mathbf{r})|^2 \qquad \mathbf{D} = \varepsilon_0\epsilon_0\mathbf{E}$$

$$\frac{1}{2}\int d\mathbf{r}\,\mathbf{E}\cdot\mathbf{D} = \frac{1}{2}\frac{e^2}{4\pi\varepsilon_0}\left(\frac{1}{\epsilon_0}\right)\int d\mathbf{r}\,d\mathbf{r}'\,\frac{|\psi(\mathbf{r})|^2|\psi(\mathbf{r}')|^2}{|\mathbf{r}-\mathbf{r}'|}$$

Pekar, Zh. Eksp. Teor. Fiz. 16, 341 (1946); Landau and Pekar, Zh. Eksp. Teor. Fiz. 18, 419 (1948)

Ground state of the polaron in the Landau-Pekar model

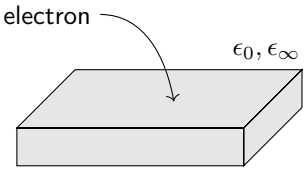

$$E = \frac{\hbar^2}{2m^*}\int d\mathbf{r}\,|\nabla\psi|^2 + \frac{1}{2}\int d\mathbf{r}\;\mathbf{E}\cdot\mathbf{D}$$

$$\nabla\cdot\mathbf{D} = -e|\psi(\mathbf{r})|^2 \qquad \mathbf{D} = \varepsilon_0\epsilon_0\mathbf{E}$$

$$\frac{1}{2}\int d\mathbf{r}\,\mathbf{E}\cdot\mathbf{D} = \frac{1}{2}\frac{e^2}{4\pi\varepsilon_0}\left(\frac{1}{\epsilon_0}-\frac{1}{\epsilon_\infty}\right)\int d\mathbf{r}\,d\mathbf{r}'\,\frac{|\psi(\mathbf{r})|^2|\psi(\mathbf{r}')|^2}{|\mathbf{r}-\mathbf{r}'|}$$

Pekar, Zh. Eksp. Teor. Fiz. 16, 341 (1946); Landau and Pekar, Zh. Eksp. Teor. Fiz. 18, 419 (1948)

Ground state of the polaron in the Landau-Pekar model

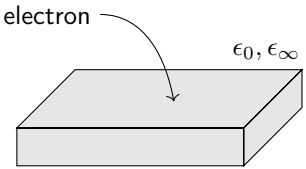

$$E = \frac{\hbar^2}{2m^*}\int d\mathbf{r}\,|\nabla\psi|^2 + \frac{1}{2}\int d\mathbf{r}\;\mathbf{E}\cdot\mathbf{D}$$

$$\nabla\cdot\mathbf{D} = -e|\psi(\mathbf{r})|^2 \qquad \mathbf{D} = \varepsilon_0\epsilon_0\mathbf{E}$$

$$\frac{1}{2}\int d\mathbf{r}\,\mathbf{E}\cdot\mathbf{D} = \frac{1}{2}\frac{e^2}{4\pi\varepsilon_0}\left(\frac{1}{\epsilon_0}-\frac{1}{\epsilon_\infty}\right)\int d\mathbf{r}\,d\mathbf{r}'\,\frac{|\psi(\mathbf{r})|^2|\psi(\mathbf{r}')|^2}{|\mathbf{r}-\mathbf{r}'|}$$

$$E[\psi(\mathbf{r})] = \frac{\hbar^2}{2m^*}\int d\mathbf{r}\,|\nabla\psi(\mathbf{r})|^2 - \frac{1}{2}\frac{e^2}{4\pi\epsilon_0}\left(\frac{1}{\epsilon_\infty}-\frac{1}{\epsilon_0}\right)\int d\mathbf{r}\,d\mathbf{r}'\,\frac{|\psi(\mathbf{r})|^2|\psi(\mathbf{r}')|^2}{|\mathbf{r}-\mathbf{r}'|}$$

Pekar, Zh. Eksp. Teor. Fiz. 16, 341 (1946); Landau and Pekar, Zh. Eksp. Teor. Fiz. 18, 419 (1948)

Variational solution for the Landau-Pekar equation

Simplest trial solution

$$\psi(\mathbf{r}) = \exp(-|\mathbf{r}|/r_{\mathrm{p}})$$

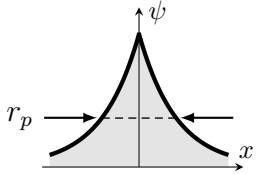

Variational solution for the Landau-Pekar equation

Simplest trial solution

$\psi(\mathbf{r}) = \exp(-|\mathbf{r}|/r_{\mathrm{p}})$

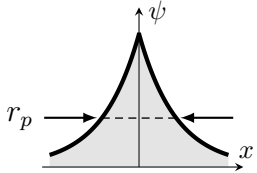

$E =$

Variational solution for the Landau-Pekar equation

Simplest trial solution

$$\psi(\mathbf{r}) = \exp(-|\mathbf{r}|/r_{\mathrm{p}})$$

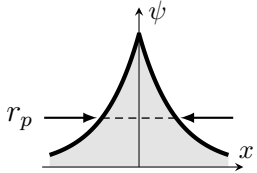

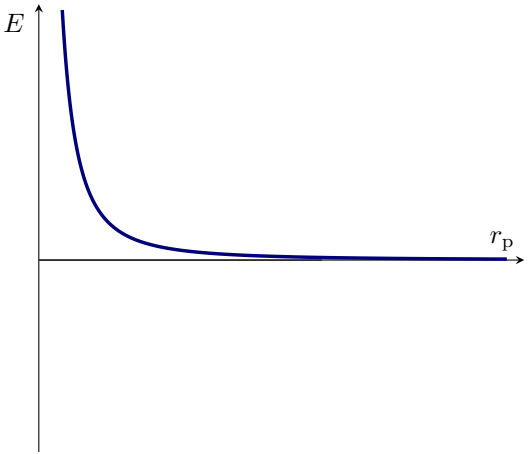

$$E = \frac{\hbar^2}{2m^*}\frac{1}{r_{\mathrm{p}}^2}$$

Variational solution for the Landau-Pekar equation

Simplest trial solution

$$\psi(\mathbf{r}) = \exp(-|\mathbf{r}|/r_\mathrm{p})$$

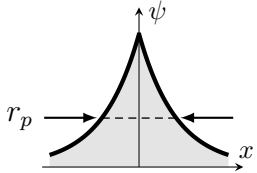

$$E = \frac{\hbar^2}{2m^*}\frac{1}{r_\mathrm{p}^2} - \frac{5}{16}\left(\frac{1}{\epsilon_0} - \frac{1}{\epsilon_\infty}\right)\frac{e^2}{4\pi\varepsilon_0}\frac{1}{r_\mathrm{p}}$$

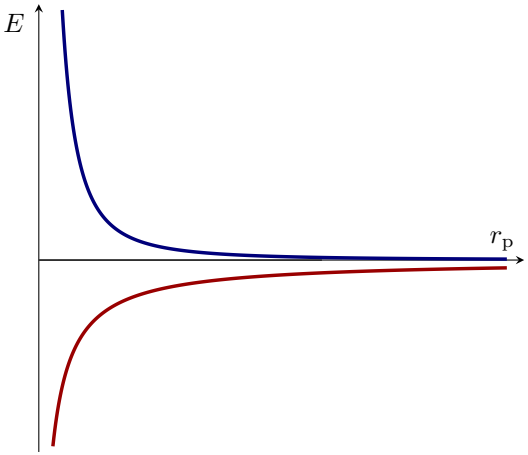

Variational solution for the Landau-Pekar equation

Simplest trial solution

$$\psi(\mathbf{r}) = \exp(-|\mathbf{r}|/r_\mathrm{p})$$

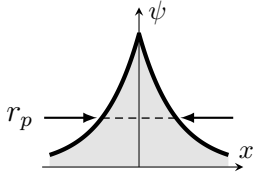

$$E = \frac{\hbar^2}{2m^*}\frac{1}{r_\mathrm{p}^2} - \frac{5}{16}\left(\frac{1}{\epsilon_0} - \frac{1}{\epsilon_\infty}\right)\frac{e^2}{4\pi\varepsilon_0}\frac{1}{r_\mathrm{p}}$$

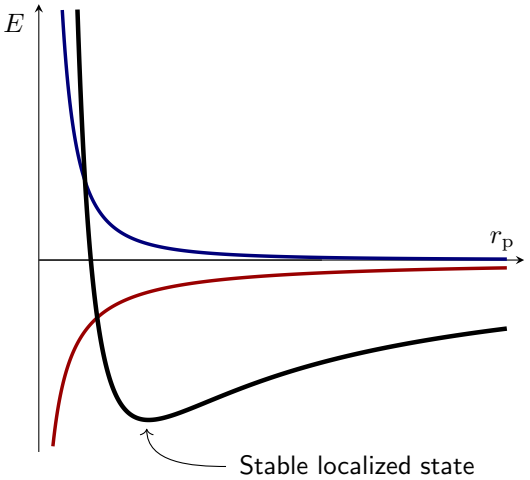

Effect of DFT self-interaction and hybrid exchange fraction

$$-\left(\frac{1}{\epsilon_\infty}-\frac{1}{\epsilon_0}\right)\int d\mathbf{r}'\,\frac{|\psi(\mathbf{r}')|^2}{|\mathbf{r}-\mathbf{r}'|}$$

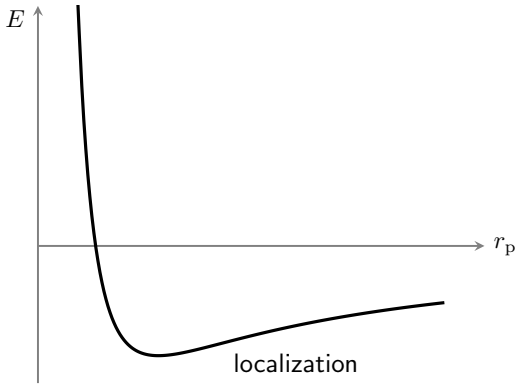

Effect of DFT self-interaction and hybrid exchange fraction

$$-\left(\frac{1}{\epsilon_\infty}-\frac{1}{\epsilon_0}\right)\int d\mathbf{r}'\,\frac{|\psi(\mathbf{r}')|^2}{|\mathbf{r}-\mathbf{r}'|} \;+\; \int d\mathbf{r}'\,\frac{|\psi(\mathbf{r}')|^2}{|\mathbf{r}-\mathbf{r}'|}$$

DFT self-interaction

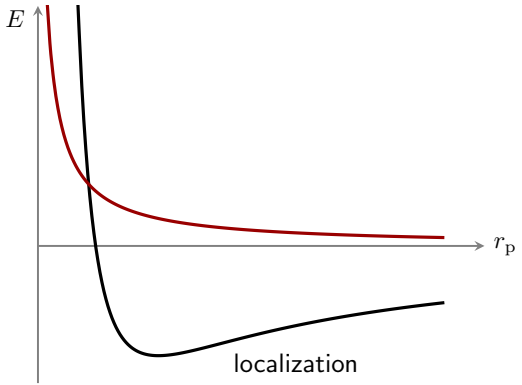

Effect of DFT self-interaction and hybrid exchange fraction

$$-\left(\frac{1}{\epsilon_\infty}-\frac{1}{\epsilon_0}\right)\int d\mathbf{r}'\,\frac{|\psi(\mathbf{r}')|^2}{|\mathbf{r}-\mathbf{r}'|} \;+\; \int d\mathbf{r}'\,\frac{|\psi(\mathbf{r}')|^2}{|\mathbf{r}-\mathbf{r}'|}$$

DFT self-interaction

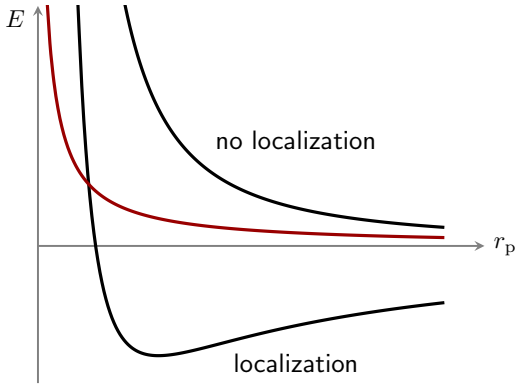

Effect of DFT self-interaction and hybrid exchange fraction

$$-\left(\frac{1}{\epsilon_\infty}-\frac{1}{\epsilon_0}\right)\int d\mathbf{r}'\,\frac{|\psi(\mathbf{r}')|^2}{|\mathbf{r}-\mathbf{r}'|} \;+\; \int d\mathbf{r}'\,\frac{|\psi(\mathbf{r}')|^2}{|\mathbf{r}-\mathbf{r}'|} \;-\; \alpha\int d\mathbf{r}'\,\frac{|\psi(\mathbf{r}')|^2}{|\mathbf{r}-\mathbf{r}'|}$$

DFT self-interaction — Fock exchange

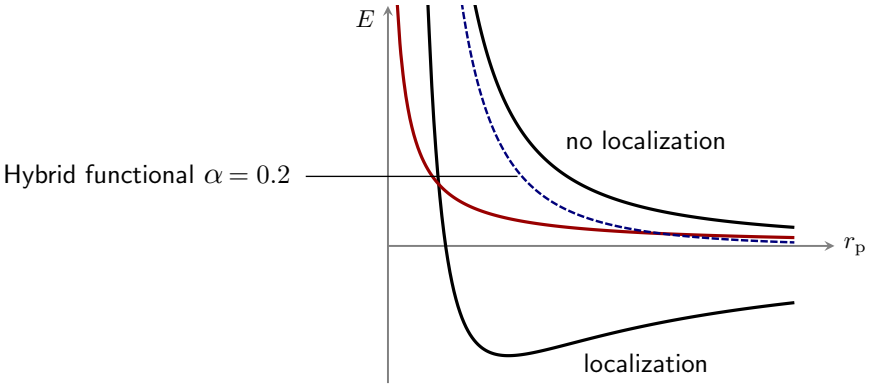

Effect of DFT self-interaction and hybrid exchange fraction

$$-\left(\frac{1}{\epsilon_\infty}-\frac{1}{\epsilon_0}\right)\int d\mathbf{r}'\,\frac{|\psi(\mathbf{r}')|^2}{|\mathbf{r}-\mathbf{r}'|} \;+\; \int d\mathbf{r}'\,\frac{|\psi(\mathbf{r}')|^2}{|\mathbf{r}-\mathbf{r}'|} \;-\; \alpha\int d\mathbf{r}'\,\frac{|\psi(\mathbf{r}')|^2}{|\mathbf{r}-\mathbf{r}'|}$$

DFT self-interaction — Fock exchange

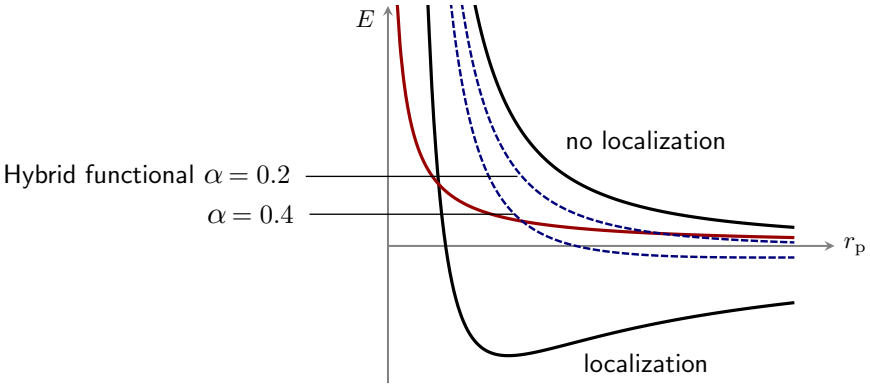

Effect of DFT self-interaction and hybrid exchange fraction

$$-\left(\frac{1}{\epsilon_\infty}-\frac{1}{\epsilon_0}\right)\int d\mathbf{r}'\,\frac{|\psi(\mathbf{r}')|^2}{|\mathbf{r}-\mathbf{r}'|} \;+\; \int d\mathbf{r}'\,\frac{|\psi(\mathbf{r}')|^2}{|\mathbf{r}-\mathbf{r}'|} \;-\; \alpha\int d\mathbf{r}'\,\frac{|\psi(\mathbf{r}')|^2}{|\mathbf{r}-\mathbf{r}'|}$$

DFT self-interaction — Fock exchange

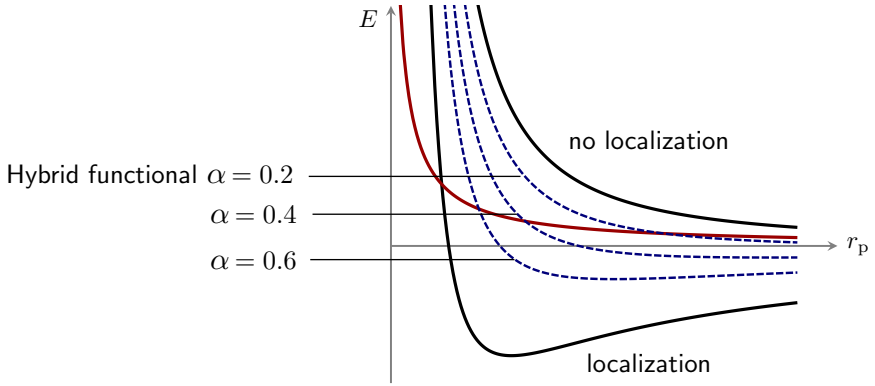

Effect of DFT self-interaction and hybrid exchange fraction

$$-\left(\frac{1}{\epsilon_\infty}-\frac{1}{\epsilon_0}\right)\int d\mathbf{r}'\,\frac{|\psi(\mathbf{r}')|^2}{|\mathbf{r}-\mathbf{r}'|} \;+\; \int d\mathbf{r}'\,\frac{|\psi(\mathbf{r}')|^2}{|\mathbf{r}-\mathbf{r}'|} \;-\; \alpha\int d\mathbf{r}'\,\frac{|\psi(\mathbf{r}')|^2}{|\mathbf{r}-\mathbf{r}'|}$$

DFT self-interaction — Fock exchange

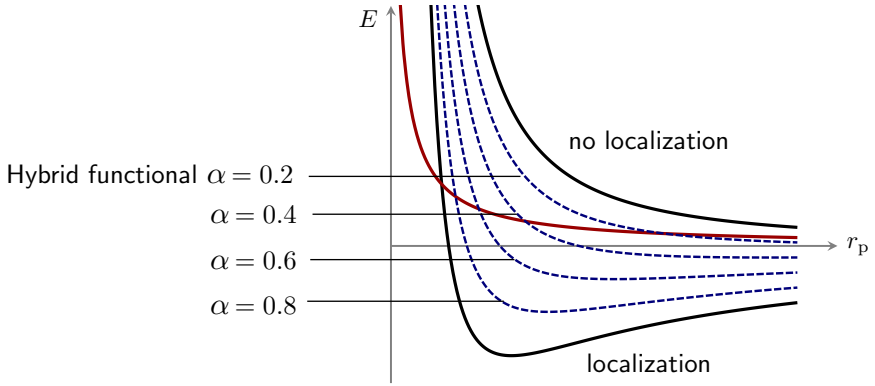

Effect of DFT self-interaction and hybrid exchange fraction

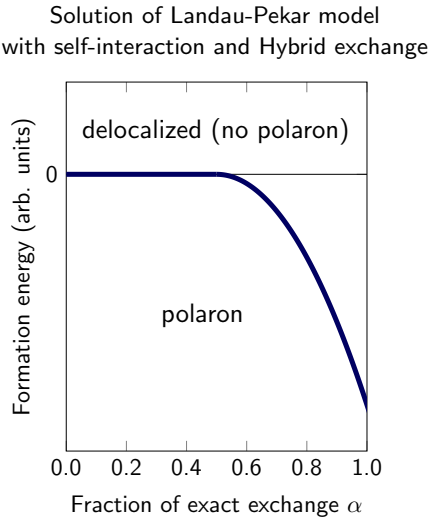

Effect of DFT self-interaction and hybrid exchange fraction

Solution of Landau-Pekar model
with self-interaction and Hybrid exchange

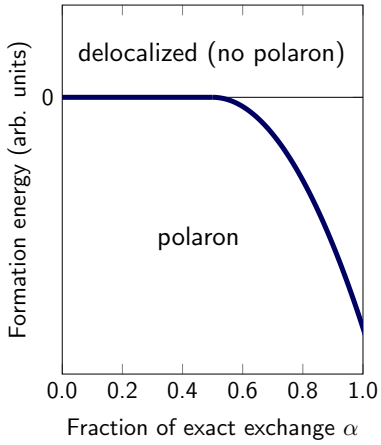

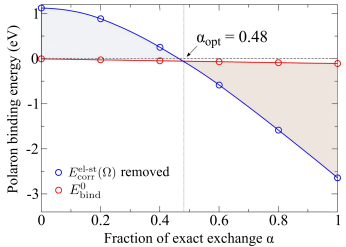

Kokott et al,
NJP 20 (2018)

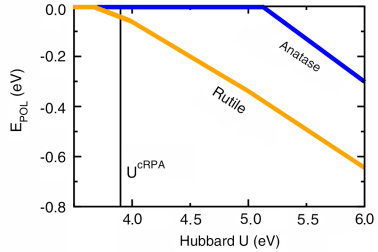

Setvin et al,
PRL 113, 086402 (2014)

Total energy in DFT

$$
\begin{aligned}
E &= \sum_{i \in \mathrm{occ}} \int d\mathbf{r} |\nabla \psi_i|^2 + \frac{1}{2} \int d\mathbf{r} d\mathbf{r}' \frac{n(\mathbf{r}) n(\mathbf{r}')}{|\mathbf{r} - \mathbf{r}'|} + E_{xc}[n] \\
&+ \sum_{\kappa} \int d\mathbf{r} \frac{Z_\kappa n(\mathbf{r})}{|\mathbf{r} - \boldsymbol{\tau}_\kappa|} + \frac{1}{2} \sum_{\kappa\kappa'} \frac{Z_\kappa Z_{\kappa'}}{|\boldsymbol{\tau}_\kappa - \boldsymbol{\tau}_{\kappa'}|}
\end{aligned}
$$

Total energy in DFT

$$
\begin{aligned}
E &= \sum_{i \in \mathrm{occ}} \int d\mathbf{r} |\nabla \psi_i|^2 + \frac{1}{2} \int d\mathbf{r} d\mathbf{r}' \frac{n(\mathbf{r}) n(\mathbf{r}')}{|\mathbf{r} - \mathbf{r}'|} + E_{xc}[n] \\
&+ \sum_{\kappa} \int d\mathbf{r} \frac{Z_\kappa n(\mathbf{r})}{|\mathbf{r} - \boldsymbol{\tau}_\kappa|} + \frac{1}{2} \sum_{\kappa\kappa'} \frac{Z_\kappa Z_{\kappa'}}{|\boldsymbol{\tau}_\kappa - \boldsymbol{\tau}_{\kappa'}|}
\end{aligned}
$$

Add one electron:

$$
\begin{cases}
n(\mathbf{r}) \longrightarrow n(\mathbf{r}) + |\psi(\mathbf{r})|^2 \\
\boldsymbol{\tau}_\kappa \longrightarrow \boldsymbol{\tau}_\kappa + \mathbf{u}_\kappa
\end{cases}
$$

Total energy in DFT

$$E \quad =$$

Total energy in DFT

$$E = \sum_{i \in \mathrm{occ}} \int d\mathbf{r} \, |\nabla \psi_i|^2 + \int d\mathbf{r} \, |\nabla \psi|^2$$

Total energy in DFT

$$
\begin{aligned}
E &= \sum_{i \in \mathrm{occ}} \int d\mathbf{r}\, |\nabla \psi_i|^2 + \int d\mathbf{r}\, |\nabla \psi|^2 \\
&+ \frac{1}{2} \int d\mathbf{r} d\mathbf{r}' \, \frac{[n(\mathbf{r}) + |\psi(\mathbf{r})|^2]\,[n(\mathbf{r}') + |\psi(\mathbf{r}')|^2]}{|\mathbf{r} - \mathbf{r}'|} + E_{xc}[n + |\psi|^2]
\end{aligned}
$$

Total energy in DFT

$$
\begin{aligned}
E &= \sum_{i \in \mathrm{occ}} \int d\mathbf{r}\, |\nabla \psi_i|^2 + \int d\mathbf{r}\, |\nabla \psi|^2 \\
&+ \frac{1}{2} \int d\mathbf{r} d\mathbf{r}' \, \frac{[n(\mathbf{r}) + |\psi(\mathbf{r})|^2]\,[n(\mathbf{r}') + |\psi(\mathbf{r}')|^2]}{|\mathbf{r} - \mathbf{r}'|} + E_{xc}[n + |\psi|^2] \\
&+ \sum_{\kappa} \int d\mathbf{r}\, \frac{Z_\kappa\, [n(\mathbf{r}) + |\psi(\mathbf{r})|^2]}{|\mathbf{r} - (\boldsymbol{\tau}_\kappa + \mathbf{u}_\kappa)\,|} + \frac{1}{2} \sum_{\kappa\kappa'} \frac{Z_\kappa Z_{\kappa'}}{|\,(\boldsymbol{\tau}_\kappa + \mathbf{u}_\kappa) - (\boldsymbol{\tau}_{\kappa'} + \mathbf{u}_{\kappa'})\,|}
\end{aligned}
$$

Total energy in DFT

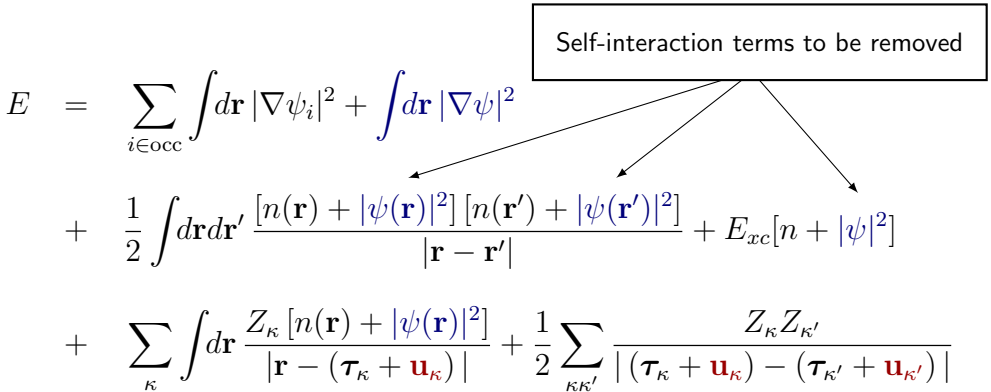

Total energy in DFT

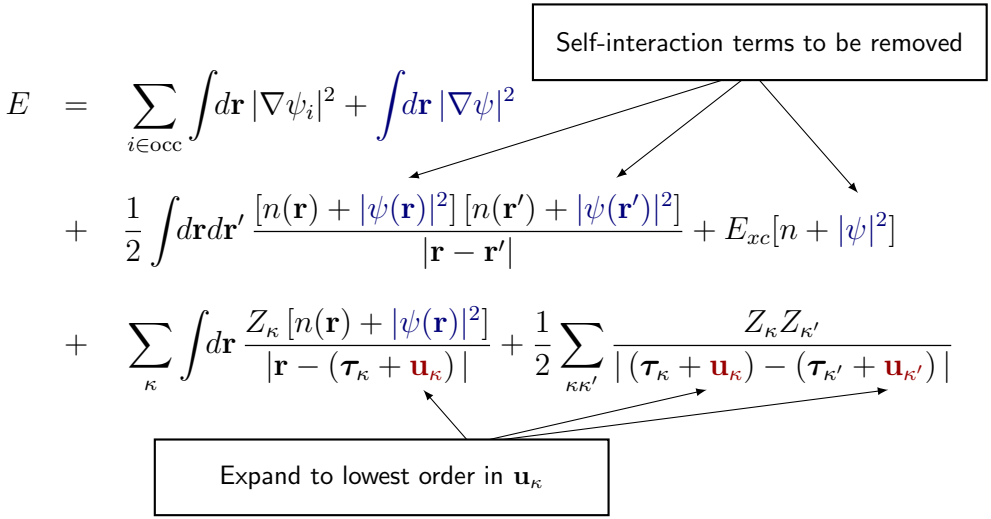

Formation energy functional of an extra electron, without self-interaction

$$E_{\mathrm{f}} = \int d\mathbf{r}\, \psi^* \hat{H}_{\mathrm{KS}}\, \psi \; + \int d\mathbf{r}\, |\psi|^2 \, \frac{\partial V_{\mathrm{KS}}}{\partial \boldsymbol{\tau}_\kappa} \cdot \mathbf{u}_\kappa + \frac{1}{2} \mathbf{u}_\kappa \cdot \mathbf{C}_{\kappa\kappa'} \cdot \mathbf{u}_{\kappa'}$$

Polarons in density-functional perturbation theory

Formation energy functional of an extra electron, without self-interaction

$$E_{\rm f} = \int d\mathbf{r}\, \psi^* \hat{H}_{\rm KS}\, \psi \; + \int d\mathbf{r}\, |\psi|^2 \, \frac{\partial V_{\rm KS}}{\partial \boldsymbol{\tau}_\kappa} \cdot \mathbf{u}_\kappa + \frac{1}{2} \mathbf{u}_\kappa \cdot \mathbf{C}_{\kappa\kappa'} \cdot \mathbf{u}_{\kappa'}$$

Variational minimization with respect to ψ and $\mathbf{u}_\kappa$ & normalization of ψ

$$\begin{cases} \hat{H}_{\rm KS}\, \psi + \; \psi \, \dfrac{\partial V_{\rm KS}}{\partial \boldsymbol{\tau}_\kappa} \cdot \mathbf{u}_\kappa = \lambda\, \psi \\ \mathbf{u}_\kappa = -(\mathbf{C})^{-1}_{\kappa\kappa'} \cdot \displaystyle\int d\mathbf{r}\, \frac{\partial V_{\rm KS}}{\partial \boldsymbol{\tau}_{\kappa'}}\, |\psi|^2 \end{cases}$$

Derivation in Sio et al, PRB 99, 235139 (2019)

Polarons in reciprocal space

$$\psi(\mathbf{r}) = \frac{1}{N_p} \sum_{n\mathbf{k}} A_{n\mathbf{k}}\, \psi_{n\mathbf{k}}(\mathbf{r})$$

$$\mathbf{u}_\kappa(\mathbf{R}) = -\frac{2}{N_p} \sum_{\mathbf{q}\nu} B^*_{\mathbf{q}\nu} \sqrt{\frac{\hbar}{2M_\kappa \omega_{\mathbf{q}\nu}}}\, e^{i\mathbf{q}\cdot\mathbf{R}}\, \mathbf{e}_{\kappa,\mathbf{q}\nu}$$

Derivation in Sio et al, PRB 99, 235139 (2019)

Polarons in reciprocal space

$$\psi(\mathbf{r}) = \frac{1}{N_p} \sum_{n\mathbf{k}} A_{n\mathbf{k}}\, \psi_{n\mathbf{k}}(\mathbf{r})$$

$$\mathbf{u}_\kappa(\mathbf{R}) = -\frac{2}{N_p} \sum_{\mathbf{q}\nu} B^*_{\mathbf{q}\nu} \sqrt{\frac{\hbar}{2M_\kappa \omega_{\mathbf{q}\nu}}}\, e^{i\mathbf{q}\cdot\mathbf{R}}\, \mathbf{e}_{\kappa,\mathbf{q}\nu}$$

$$\frac{2}{N_p} \sum_{\mathbf{q}m\nu} B_{\mathbf{q}\nu}\, g^*_{mn\nu}(\mathbf{k},\mathbf{q})\, A_{m\mathbf{k}+\mathbf{q}} = (\varepsilon_{n\mathbf{k}} - \varepsilon)\, A_{n\mathbf{k}}$$

$$B_{\mathbf{q}\nu} = \frac{1}{N_p} \sum_{mn\mathbf{k}} A^*_{m\mathbf{k}+\mathbf{q}}\, \frac{g_{mn\nu}(\mathbf{k},\mathbf{q})}{\hbar\omega_{\mathbf{q}\nu}}\, A_{n\mathbf{k}}$$

Ab initio polaron equations

Derivation in Sio et al, PRB 99, 235139 (2019)

Example: Excess electron in LiF

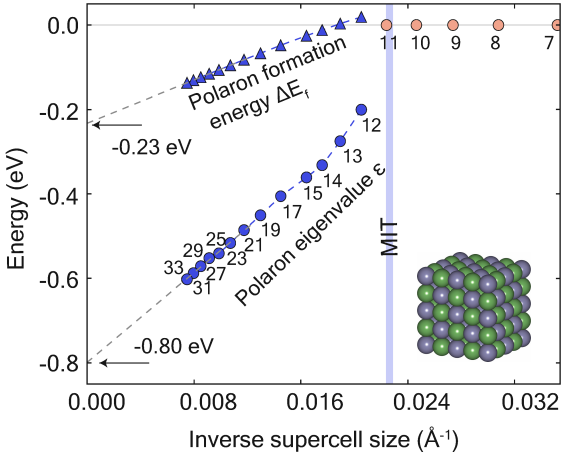

Example: Excess electron in LiF

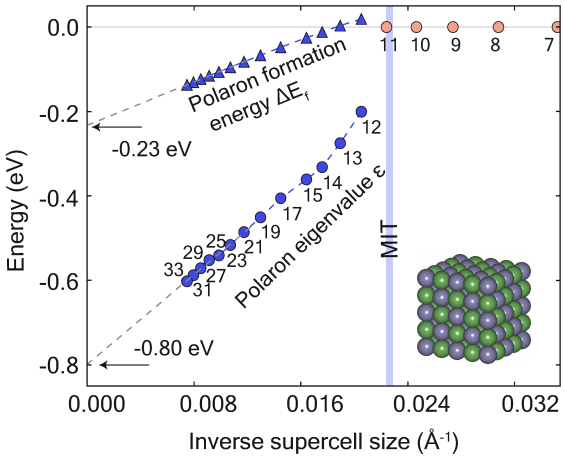

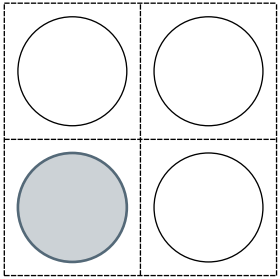

Low density

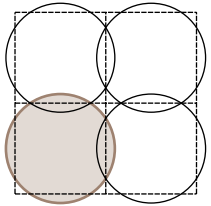

High density

Example: Excess electron in LiF

→ Tut. Fri.5 Lafuente

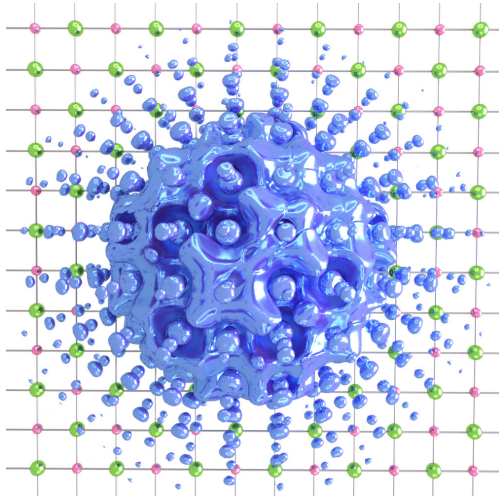

3,456 atoms

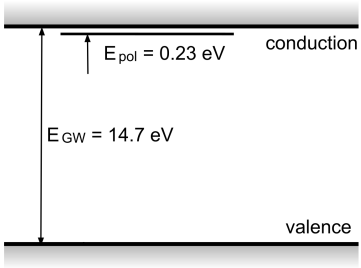

Figure from Sio et al, Phys. Rev. B 99, 235139 (2019)

Example: Excess electron in LiF

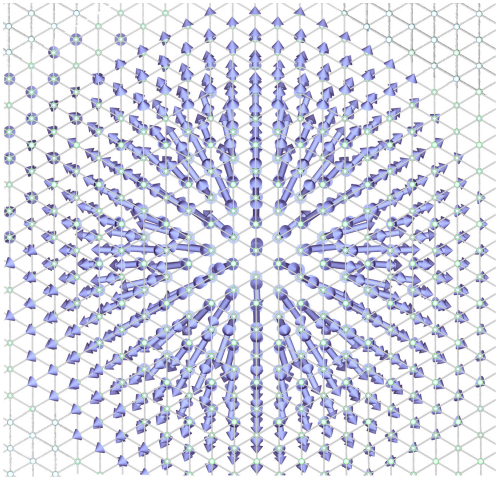

3,456 atoms

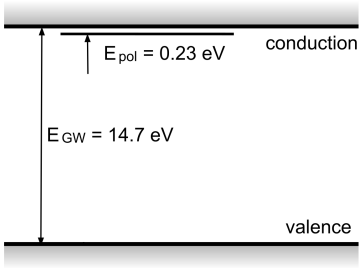

Figure from Sio et al, Phys. Rev. B 99, 235139 (2019)

Example: Excess hole in LiF

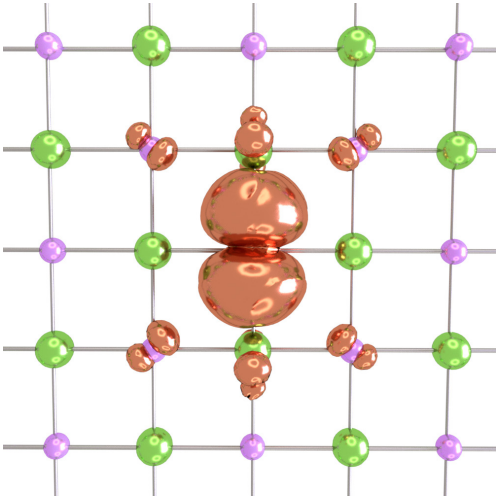

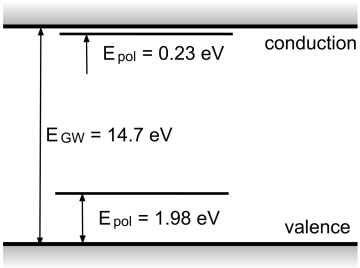

Figure from Sio et al, Phys. Rev. B 99, 235139 (2019)

Polaron as coherent superposition of Bloch waves

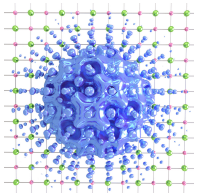

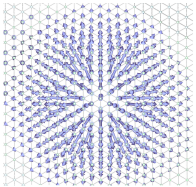

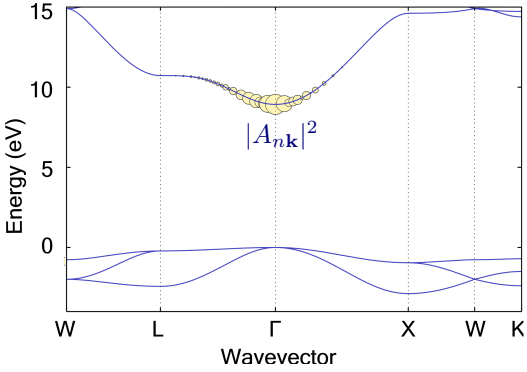

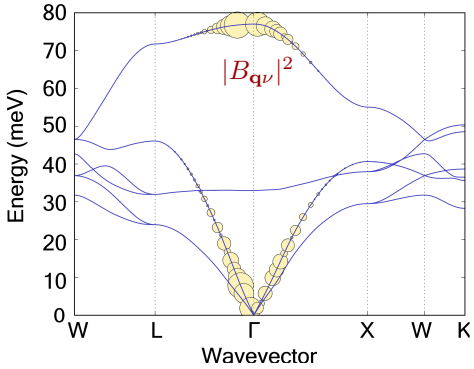

Polaron transport: Hopping barrier in $Cs_2AgBiBr_6$

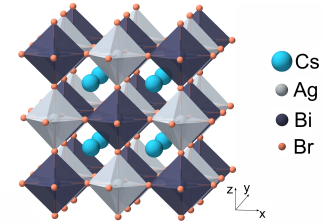

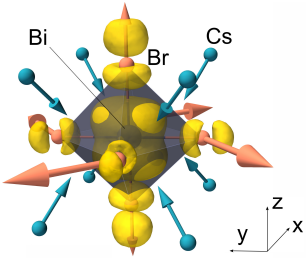

Figures from Lafuente-Bartolomé et al, PNAS 121, e2318151121 (2024)

Polaron transport: Hopping barrier in $Cs_2AgBiBr_6$

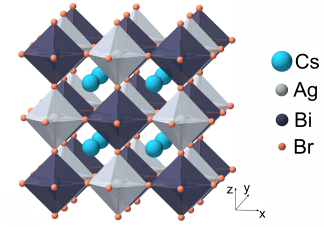

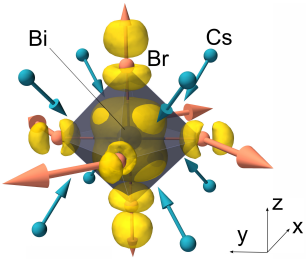

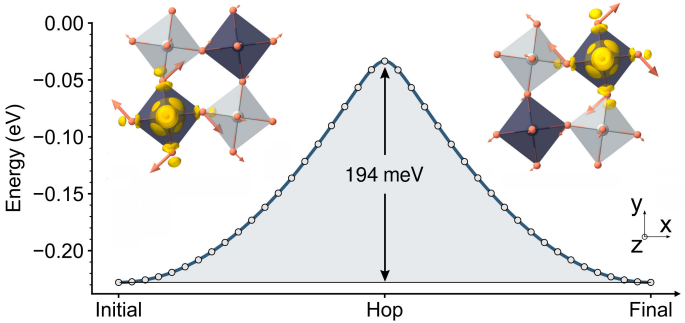

Figures from Lafuente-Bartolomé et al, PNAS 121, e2318151121 (2024)

Anisotropic polarons: Thermoelectric SnSe

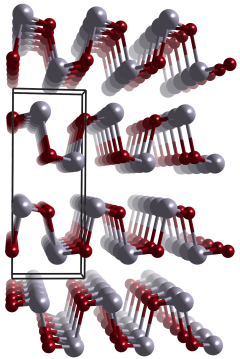

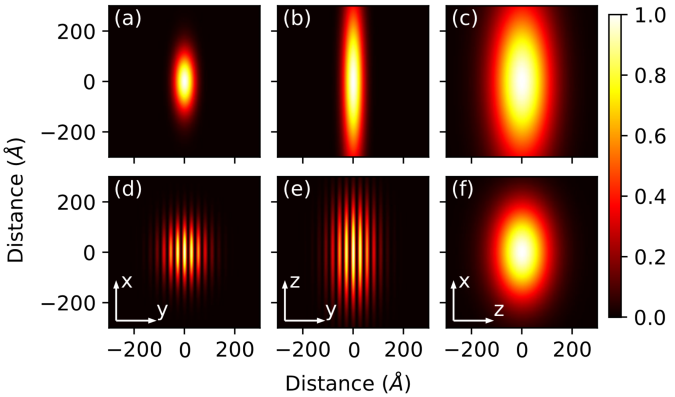

Right figure from Guster, Gonze, et al, Phys. Rev. Mater. 7, 064604 (2023)

Left figure from en.wikipedia.org/wiki/Tin_selenide

Polarons in 2D materials: Monolayer h-BN

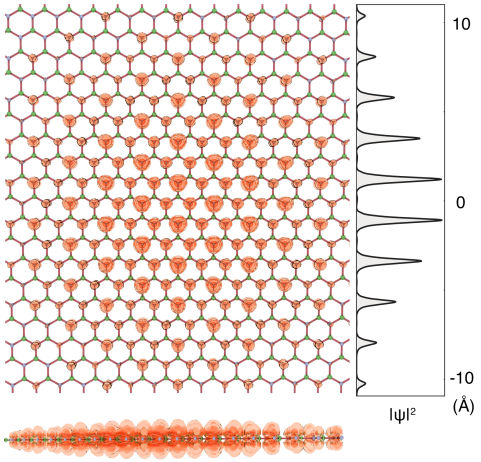

2D EPC matrix elements:

→ Lec. Wed.1 Poncé

→ Tut. Wed.5 Ha

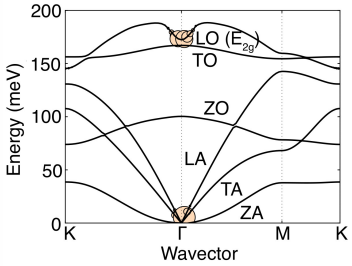

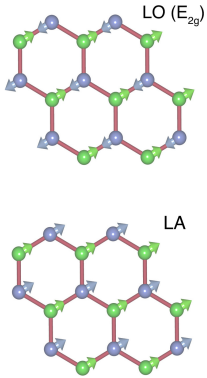

Figure from Sio et al, Nat. Phys. 19, 629 (2023)

Relation with the many-body formulation of Lec. Tue.2

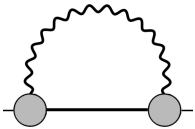

Fan-Migdal self-energy

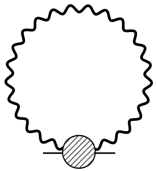

Debye-Waller self-energy

Derivation in Lafuente-Bartolomé et al, Phys. Rev. B 106, 075119 (2022)

See also tadpole self-energy in Marini et al, Phys. Rev. B 91, 224310 (2015)

Relation with the many-body formulation of Lec. Tue.2

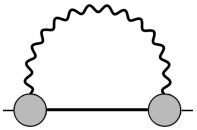

Fan-Migdal self-energy

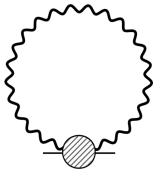

Debye-Waller self-energy

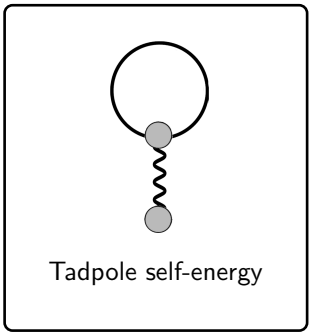

Tadpole self-energy

Derivation in Lafuente-Bartolomé et al, Phys. Rev. B 106, 075119 (2022)

See also tadpole self-energy in Marini et al, Phys. Rev. B 91, 224310 (2015)

Relation with the many-body formulation of Lec. Tue.2

Path integral approach to the **Fröhlich model**: Feynman, Phys. Rev. 97, 660 (1955)

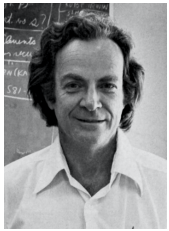

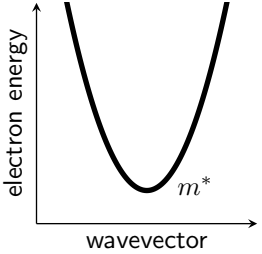

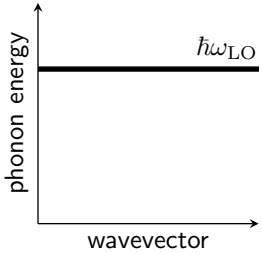

$$g(q) = \frac{\hbar\omega_{\mathrm{LO}}}{l}\frac{\sqrt{\alpha}}{q}$$

Relation with the many-body formulation of Lec. Tue.2

Path integral approach to the **Fröhlich model**: Feynman, Phys. Rev. 97, 660 (1955)

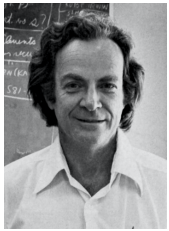

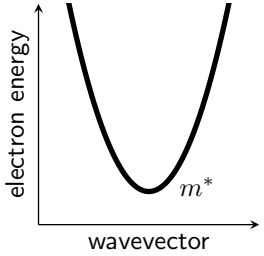

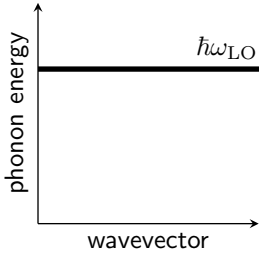

$$g(q) = \frac{\hbar\omega_{\mathrm{LO}}}{l}\frac{\sqrt{\alpha}}{q}$$

Fröhlich coupling constant

$$\alpha = \frac{e^2}{4\pi\epsilon_0\hbar}\sqrt{\frac{m^*}{2\hbar\omega_{\mathrm{LO}}}}\left(\frac{1}{\epsilon^\infty} - \frac{1}{\epsilon^0}\right)$$

Characteristic length

$$l = \sqrt{\frac{\Omega}{2\sqrt{2}\pi}\sqrt{\frac{m^*\omega_{\mathrm{LO}}}{\hbar}}}$$

Relation with the many-body formulation of Lec. Tue.2

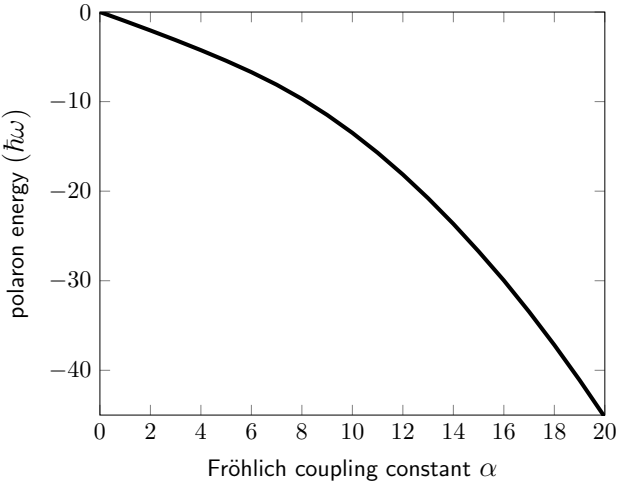

Relation with the many-body formulation of Lec. Tue.2

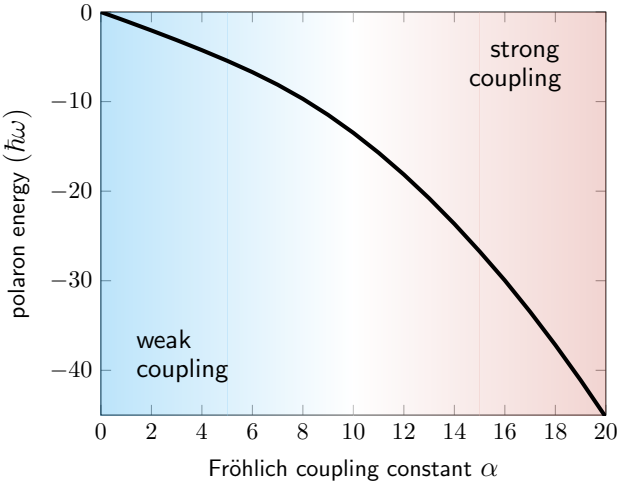

Relation with the many-body formulation of Lec. Tue.2

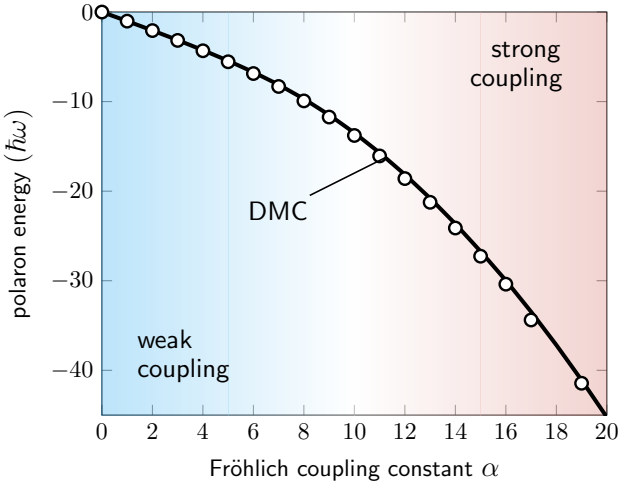

Diagrammatic Monte Carlo data from Hahn, Franchini et al, Phys. Rev. B 97, 134305 (2018)

Relation with the many-body formulation of Lec. Tue.2

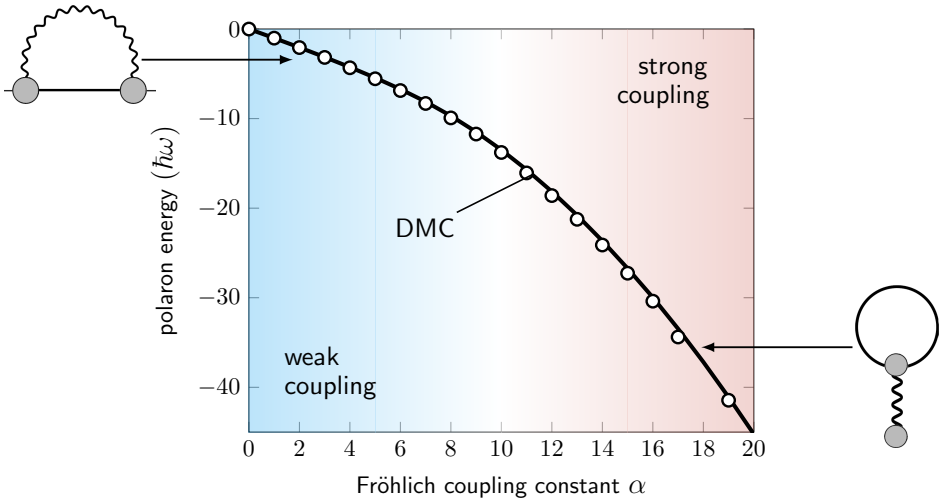

Diagrammatic Monte Carlo data from Hahn, Franchini et al, Phys. Rev. B 97, 134305 (2018)

Many-body field-theoretic approach to polarons

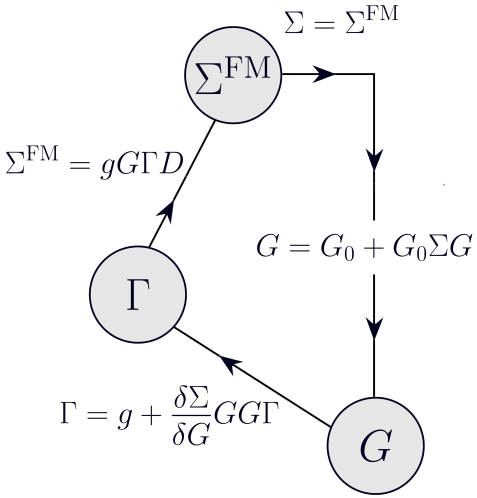

Figure from Lafuente-Bartolomé et al, Phys. Rev. Lett. 129, 076402 (2022)

Many-body field-theoretic approach to polarons

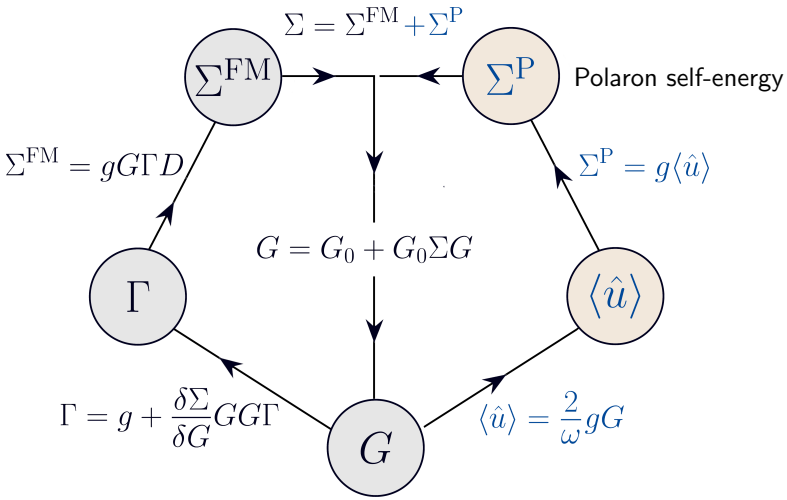

Figure from Lafuente-Bartolomé et al, Phys. Rev. Lett. 129, 076402 (2022)

Many-body field-theoretic approach to polarons

Lehmann representation of the Green's function

$$G(\mathbf{r},\mathbf{r}';\omega)=\sum_s \frac{f_s(\mathbf{r})f_s^*(\mathbf{r}')}{\hbar\omega-\varepsilon_s} \longrightarrow$$

Dyson orbitals

$$f_s(\mathbf{r})=\frac{1}{\sqrt{N}}\sum_{n\mathbf{k}} A^s_{n\mathbf{k}}\,\psi_{n\mathbf{k}}(\mathbf{r})$$

From Lafuente-Bartolomé at al, PRB 106, 075119 (2022)

Many-body field-theoretic approach to polarons

Lehmann representation of the Green's function

$$G(\mathbf{r},\mathbf{r}';\omega) = \sum_s \frac{f_s(\mathbf{r}) f_s^*(\mathbf{r}')}{\hbar\omega - \varepsilon_s} \longrightarrow f_s(\mathbf{r}) = \frac{1}{\sqrt{N}} \sum_{n\mathbf{k}} A^s_{n\mathbf{k}}\, \psi_{n\mathbf{k}}(\mathbf{r})$$

Dyson orbitals

$$\sum_{n'\mathbf{k}'} \left[\varepsilon_{n\mathbf{k}}\, \delta_{n\mathbf{k},n'\mathbf{k}'} + \Sigma^{\mathrm{FM}}_{n\mathbf{k},n'\mathbf{k}'}(\varepsilon_s) + \Sigma^{\mathrm{P}}_{n\mathbf{k},n'\mathbf{k}'} \right] A^s_{n'\mathbf{k}'} = \varepsilon_s\, A^s_{n\mathbf{k}}$$

Many-body *ab initio* polaron equations

From Lafuente-Bartolomé at al, PRB 106, 075119 (2022)

Exciton polarons

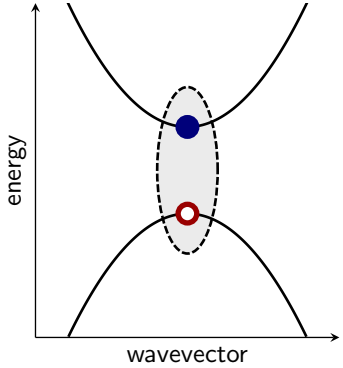

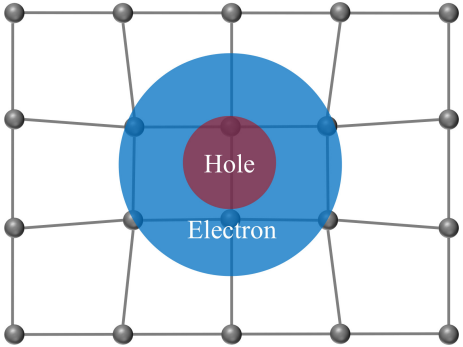

→ Lec. Fri.4 Dai

Take-home messages

- DFT calculations of polarons suffer from self-interaction error
- *Ab initio* polaron equations yield self-interaction-free energies and wavefunctions
- Polarons can be studies using many-body Green's functions as in Lec. Tue.2
- There are many types of polarons, from very small to very large

Further reading

- Franchini, Reticcioli, Setvin, and Diebold, Nat. Rev. Mater. 6, 560 (2021) [link]
- Sio, Verdi, Poncé, and Giustino, Phys. Rev. B 99, 235139 (2019) [link]
- Lafuente-Bartolomé, Lian, Sio, Guturbay, Eiguren, and Giustino, Phys. Rev. B 106, 075119 (2022) [link]
- Devreese and Alexandrov, Rep. Prog. Phys. 72, 066501 (2009) [link]
- Devreese, arXiv:1611.06122 (2020) [link]
- Lee, Chen, Zhou, and Bernardi, Phys. Rev. Materials 5, 063805 (2021) [link]
- Falletta and Pasquarello, Phys. Rev. B 106, 125119 (2022) [link]